

# Functional Characterization of an Endosome-disruptive Peptide and Its Application in Cytosolic Delivery of Immunoliposome-entrapped Proteins\*

Received for publication, January 15, 2002, and in revised form, April 24, 2002  
Published, JBC Papers in Press, May 20, 2002, DOI 10.1074/jbc.M200429200

Enrico Mastrobattista, Gerben A. Koning, Louis van Bloois, Ana C. S. Filipe, Wim Jiskoot, and Gert Storm‡

From the Department of Pharmaceutics, Utrecht University, P.O. Box 80 082, Utrecht 3508 TB, The Netherlands

**Antibody-directed liposomes (immunoliposomes) are frequently used for targeted drug delivery. However, delivery of large biotherapeutic molecules (i.e. peptides, proteins, or nucleic acids) with immunoliposomes is often hampered by an inefficient cytosolic release of entrapped macromolecules after target cell binding and subsequent endocytosis of immunoliposomes. To enhance cytosolic drug delivery from immunoliposomes present inside endosomes, a pH-dependent fusogenic peptide (diINF-7) resembling the NH<sub>2</sub>-terminal domain of influenza virus hemagglutinin HA-2 subunit was used. Functional characterization of this dimeric peptide showed its ability to induce fusion between liposome membranes and leakage of liposome-entrapped compounds when exposed to low pH. In a second series of experiments, diINF-7 peptides were encapsulated in immunoliposomes to enhance the endosomal escape of diphtheria toxin A chain (DTA), which inhibits protein synthesis when delivered into the cytosol of target cells. Immunoliposomes targeted to the internalizing epidermal growth factor receptor on the surface of ovarian carcinoma cells (OVCAR-3) and containing encapsulated DTA did not show any cytotoxicity toward OVCAR-3 cells. Cytotoxicity was only observed when diINF-7 peptides and DTA were co-encapsulated in the immunoliposomes. Thus, diINF-7 peptides entrapped inside liposomes can greatly enhance cytosolic delivery of liposomal macromolecules by pH-dependent destabilization of endosomal membranes after cellular uptake of liposomes.**

To exert an optimal therapeutic effect, an administered drug must safely reach not only its target cell but also the appropriate location within that cell. Many biotherapeutic agents (e.g. peptides, proteins, and nucleic acids) act at sites in the cytosol or nucleus that are difficult to reach due to poor membrane permeation characteristics. Therefore, these biotherapeutic agents rely on drug carriers that allow cytosolic delivery of these agents into diseased cells.

One attractive strategy to obtain cytosolic delivery is the development of fusion-competent antibody-directed liposomes (immunoliposomes) that, after receptor binding, can fuse with the plasma-membrane of target cells or, after endocytosis of liposomes, with the endosomal membranes. This membrane

fusion process should result in cytosolic access of liposome-entrapped drug molecules. Such fusion-competent liposomes can be obtained by disassembling enveloped viruses, isolating their fusion-promoting components, and reassembling these into vesicles to obtain so-called virosomes (1–4). Another, more refined approach involves the use of synthetic peptides designed to resemble the putative fusion peptide of viruses (5–8). It is hypothesized that destabilization of endosomal membranes is less damaging than plasma membrane destabilization. The latter may result in cytotoxicity through eradication of the electrochemical potential generated by the asymmetric distribution of ions across the plasma membrane. Therefore, drug delivery into the cytosol of target cells via endosomal escape is the preferred route. It is expected that fusion and/or membrane-destabilizing mechanisms that allow endosomal escape of liposome-entrapped therapeutic macromolecules will increase the therapeutic availability at the intracellular target site and, consequently, the therapeutic efficacy of liposomal drug formulations.

Many viral fusion peptides have been identified. Their mechanistic and structural role in the fusion process occurring between the envelopes of viruses and membranes of host cells has been extensively studied, both with intact viral fusion proteins and with synthetic analogs of the fusion protein domains. One of the best characterized viral fusion peptides is the NH<sub>2</sub>-terminal domain of influenza virus hemagglutinin subunit HA-2 (9, 10). Recently, the membrane structure of the NH<sub>2</sub>-terminal fusion domain of influenza virus hemagglutinin and the low pH-induced conformational change has been resolved by NMR (11). It was demonstrated that synthetic analogs of the hemagglutinin fusion domain attached to a hydrophilic sequence inserted into liposomal bilayers in an “inverted V” conformation both at neutral (pH 7.4) and acidic pH (pH 5.0) with residue 12 located at the bilayer surface. At pH 5.0, at which the peptide is rendered fusogenic, the COOH-terminal side of the V-shaped peptide undergoes a conformational change, resulting in the formation of short 3<sub>10</sub>-helix, that allows steeper insertion of the fusion peptide into the bilayer. This steeper insertion is thought to cause membrane destabilization.

Studies with synthetic peptides resembling the native sequence of the influenza virus NH<sub>2</sub>-terminal domain of the HA-2 subunit have clearly demonstrated that such peptides are able to destabilize both model membranes (such as liposomes) and natural membranes in a pH-dependent manner. Fusion peptide-induced lipid mixing and aqueous content mixing between liposomes have been demonstrated, indicating that the peptide analogues have fusogenic capacities (12, 13). Influenza virus-derived fusion peptides have been used to enhance the endosomal escape of oligonucleotides (14, 15) and polycation-condensed DNA complexes (5, 16, 17) after cellular uptake.

\* The costs of publication of this article were defrayed in part by the payment of page charges. This article must therefore be hereby marked “advertisement” in accordance with 18 U.S.C. Section 1734 solely to indicate this fact.

‡ To whom correspondence should be addressed. Tel.: 31-30-2537388; Fax: 31-30-2517839; E-mail: g.storm@pharm.uu.nl.

Surprisingly, despite the wealth of reports on the use of liposomes to functionally characterize fusogenic peptides, only one study reported on the utility of these peptides in enhancing cytosolic delivery of liposome-entrapped drugs (18).

In this paper, the possibility to utilize co-encapsulation of pH-dependent fusion peptides into liposomal drug formulations as a means to obtain endosomal escape of liposome-entrapped drug molecules and release of these molecules into the cytosol of tumor cells was studied. For this purpose, a dimeric peptide (diINF-7) resembling the NH<sub>2</sub>-terminal domain of influenza virus hemagglutinin was synthesized. A previous study demonstrated that the use of a dimer is preferred, since dimerization resulted in a strongly increased destabilizing activity toward liposomal bilayers and erythrocytes (10). First, the membrane-destabilizing and fusogenic capacity of diINF-7 either in free form or encapsulated in liposomes was demonstrated by using liposomes as model membranes. Next, the capacity of these peptides to induce endosomal escape of immunoliposome-entrapped bioactive molecules was demonstrated by measuring cytosolic delivery of diphtheria toxin A chain (DTA)<sup>1</sup> as a model compound. Co-encapsulation of diINF-7 into DTA-containing immunoliposomes resulted in drastically increased cytotoxicity toward ovarian carcinoma cells, indicating that this peptide can be used to obtain cytosolic delivery of liposome-entrapped drugs with poor membrane permeation capacities.

#### EXPERIMENTAL PROCEDURES

**Materials**—Cholesterol (CHOL), 2',7'-[bis(carboxymethyl)amino]methyl-fluorescein (calcein), *N*-succinimidyl-*S*-acetylthioacetate (SATA), and sodium 3'-[1-(phenylaminocarbonyl)-3,4-tetrazolium]-bis(4-methoxy-6-nitro)benzene sulfonic acid hydrate (XTT) were obtained from Sigma. Egg phosphatidylcholine and 1,2-distearoyl-glycero-3-phosphoethanolamine-*N*-[poly(ethylene glycol) 2000] (PEG2000-DSPE) were from Avanti Polar Lipids (Birmingham, AL). Maleimide-PEG2000-DSPE was obtained from Shearwater Polymers (Huntsville, AL). 1-Hexadecanoyl-2-(1-pyrenedecanoyl)-*sn*-glycero-3-phosphocholine (PyrPC) and 1,1'-dioctadecyl-3,3,3',3'-tetramethylindodicarbocyanine, 4-chlorobenzenesulfonate salt (DiD) were purchased from Molecular Probes Europe BV (Leiden, The Netherlands). Iso-octylphenoxy-polyethoxyethanol (Triton X-100) was obtained from BDH Laboratory Supplies (Poole, UK). Dithiothreitol was from Pierce. Formaldehyde solution was obtained from Janssen Chimica (Geel, Belgium). Murine mAb 425 of isotype IgG2a (EMD55900) (Merck) directed against the human epidermal growth factor receptor (EGFR) was kindly donated by Dr. G. A. van Dongen (Department of Otolaryngology/Head and Neck Surgery, University Hospital Vrije Universiteit, Amsterdam, The Netherlands). Irrelevant isotype-matched murine mAb directed against the influenza virus HA (clone 12CA5) was kindly donated by E. Boot (Immunology Division, Department of Infectious Diseases and Immunology, Faculty of Veterinary Medicine, Utrecht University, Utrecht, The Netherlands).

**Cell Culture**—The human ovarian carcinoma cell line NIH:OVCAR-3 originated from the laboratory of Dr. Hamilton (National Cancer Institute, Bethesda, MD) (19). OVCAR-3 cells were cultured in Dulbecco's modified Eagle's medium containing 3.7 g/liter sodium bicarbonate, 4.5 g/liter L-glucose and supplemented with L-glutamine (2 mM), HEPES (10 mM), 10% (v/v) fetal calf serum, penicillin (100 IU/ml), streptomycin

(100 µg/ml), and amphotericin B (0.25 µg/ml) at 37 °C with 5% CO<sub>2</sub> in humidified air. All cell culture-related material was obtained from Invitrogen.

**Peptide Synthesis**—The 24-amino acid peptide INF-7 was synthesized by standard Fmoc (*N*-(9-fluorenyl)methoxycarbonyl) solid phase synthesis essentially as described by Plank *et al.* (20). Crude peptide was precipitated by the dropwise addition of ether and collected by centrifugation. The peptide was washed three times with ether and subsequently dried under a stream of argon followed by high vacuum. Subsequently, the peptide was dissolved in 1 ml of 20 mM ammonium bicarbonate, pH 8.5, and freeze-dried. Lyophilized peptide was stored at -20 °C. Purity and identity of the peptide were confirmed by high pressure liquid chromatography (Waters 486; Millipore Corp.), amino acid analysis, and fast atom bombardment mass spectrometry. The presence of a cysteine residue at the carboxyl terminus resulted in dimerization of the INF-7 peptide by disulfide bond formation.

**DTA Purification**—DTA was produced essentially as described by Oeltmann and Wiley (21) and Carroll *et al.* (22). In short, supernatant of cultures of *Corynebacterium diphtheriae* containing high amounts of diphtheria toxin (DT), which was kindly donated by Dr. Kersten (The National Institute of Public Health and The Environment, Bilthoven, The Netherlands) was dialyzed against two 1-liter changes of HEPES-buffered salt solution (HBS; 5 mM HEPES, 150 mM NaCl, pH 7.4) overnight at 4 °C using Slide-A-Lyzer dialysis cassettes (Pierce) with a molecular weight cut-off of 10,000. Four milligrams of dialyzed DT was nicked with trypsin (1 µg/ml in HBS) for 30 min at room temperature, after which the trypsin was inactivated with soybean trypsin inhibitor (5 µg/ml final concentration). DT was reduced and denatured in HBS containing 8 M urea and 0.1 M dithiothreitol and applied to a 1.5 × 50-cm column of Sephacryl S-200 equilibrated in elution buffer (50 mM Tris-HCl, 2 M urea, 10 mM dithiothreitol, and 1 mM EDTA, pH 7.5). Fractions of 5 ml were collected and analyzed for the presence of DTA by SDS-PAGE under reducing conditions. Fractions containing DTA were pooled and dialyzed overnight at 4 °C against two 1-liter changes of HBS containing 0.1 M 2,2'-dihydroxyethyl disulfide to reversibly block the free sulfhydryl groups. The concentration of DTA was determined spectrometrically, *versus* appropriate blanks, using the extinction coefficient at 280 nm of 1.5 liters × g<sup>-1</sup> × cm<sup>-1</sup>. The biological activity of DTA to inhibit protein synthesis was determined with a rabbit reticulocyte lysate *in vitro* translation system (Promega, Madison, WI) (23).

**Liposome Preparation and Characterization**—Lipids used for all liposome preparations were dissolved in CHCl<sub>3</sub>/MeOH (2:1 (v/v) ratio) and stored at -20 °C under a nitrogen atmosphere. Egg PC and CHOL (30 µmol of lipid) dissolved in the organic solvent were mixed at a molar ratio of 2:1 in a round bottom flask. When indicated, 0.1 mol % (relative to PL) of the lipidic fluorescence probe DiD, 10 mol % PyrPC (relative to PL), or varying amounts of PEG2000-DSPE were added to the lipid mixture prior to solvent evaporation using a rotary evaporator device. The formed lipid films were further dried under a stream of nitrogen for at least 1 h to remove traces of organic solvent. Lipid films were hydrated with 1-ml solutions of HBS, calcein (90 mM), diINF-7 (500 µg/ml in HBS), DTA (250 µg/ml in HBS), or combinations of the latter two substances. Hydration of lipids was facilitated by shaking the flasks in the presence of glass beads. The formed liposomes were subsequently extruded through polycarbonate filters with pore sizes varying from 0.05 to 0.6 µm using a hand extruder from Avanti Polar Lipids. Nontrapped material was removed from liposomes by centrifugation steps (two 45-min steps at 100,000 × g; 4 °C). Pelleted liposomes were resuspended in 1 ml of HBS. The phospholipid concentration of liposome formulations was determined by the colorimetric method of Fiske and Subbarow (24). The amount of encapsulated protein (DTA and diINF-7) was determined with the BCA protein assay reagent kit (Pierce) after disruption of the liposomes with 0.5% (v/v) Triton X-100.

**Immunoliposome Preparation**—For targeting purposes, conjugates of mAb 425-PEG2000-DSPE were transferred to liposomes essentially as described by Ishida *et al.* (25). In short, 2.5 mg of mAb 425 was modified with an 8-fold molar excess of SATA to randomly introduce thiol groups. SATA-modified mAb 425 was deacetylated and allowed to react with micelles containing PEG2000-DSPE and maleimide-PEG2000-DSPE at a 4:1 molar ratio. One micromole of liposomes was incubated with 425-PEG-DSPE micelles corresponding to an amount of 30 µg of conjugated protein for 90 min at 40 °C to allow transfer of mAb 425-PEG2000-DSPE to the liposomes. Purification of liposomes was performed on a Sepharose CL-4B column (Amersham Biosciences). With this technique, ~70% of targeting ligands could be reproducibly transferred into preformed liposomes.

<sup>1</sup> The abbreviations used are: DTA, diphtheria toxin A chain; CHOL, cholesterol; calcein, 2',7'-[bis(carboxymethyl)amino]methyl-fluorescein; SATA, *N*-succinimidyl-*S*-acetylthioacetate; XTT, sodium 3'-[1-(phenylaminocarbonyl)-3,4-tetrazolium]-bis(4-methoxy-6-nitro)benzene sulfonic acid hydrate; PEG, poly(ethylene glycol) 2000; PEG2000-DSPE, 1,2-distearoyl-glycero-3-phosphoethanolamine-*N*-[poly(ethylene glycol) 2000]; PyrPC, 1-hexadecanoyl-2-(1-pyrenedecanoyl)-*sn*-glycero-3-phosphocholine; DiD, 1,1'-dioctadecyl-3,3,3',3'-tetramethylindodicarbocyanine, 4-chlorobenzenesulfonate salt; Triton X-100, iso-octylphenoxy-polyethoxyethanol; mAb, monoclonal antibody; EGFR, epidermal growth factor receptor; DT, diphtheria toxin; HBS, HEPES-buffered salt solution; PC, phosphatidylcholine; PL, phospholipid; Mes, 2-[*N*-morpholino]ethanesulfonic acid; EPC, egg-derived phosphatidylcholine; CLSM, confocal laser scanning microscopy.

**Flow Cytometry and Confocal Laser-scanning Microscopy Analysis**—OVCAR-3 cells grown to a confluent monolayer were detached from culture flasks by incubating the cells for 5 min at 37 °C with trypsin/EDTA solutions from Invitrogen. Detached OVCAR-3 cells ( $2 \times 10^5$  cells) were incubated with DiD-labeled liposomes in a final volume of 300  $\mu$ l of culture medium for 1 h at 37 °C. Thereafter, cells were washed with immunofluorescence buffer (1% bovine serum albumin in phosphate-buffered saline, pH 7.4) by two centrifugation steps (5 min at  $750 \times g$ ) and resuspended into 500  $\mu$ l of immunofluorescence buffer before being analyzed by flow cytometry with a FACSCalibur flow cytometer (Becton & Dickinson, Mountain View, CA). For confocal laser-scanning microscopy analysis, cells that were incubated with liposomes were washed three times with 1 ml of phosphate-buffered saline before fixation with 2% (v/v) of formaldehyde in phosphate-buffered saline for 20 min at room temperature. After fixation, cells that were adhered to chamber slides were washed twice with phosphate-buffered saline and overlaid with cover slides that were sealed with nail polish. Cells were analyzed on a Leica TCS-SP confocal laser-scanning microscope equipped with a 488-nm argon, 568-nm krypton, and 647-nm HeNe laser.

**CD Measurements**—CD measurements were performed with a dual-beam DSM 1000 CD spectrophotometer (On-Line Instrument Systems, Bogart, GA). The subtractive double-grating monochromator was equipped with a fixed disk, holographic gratings (2400 lines/mm, blaze wavelength 230 nm), and 1.24-mm slits. Cuvettes with a path length of 1 mm were used, and the peptide concentration was 100  $\mu$ g/ml. CD spectra were recorded from 250 to 200 nm at 25 °C. Each measurement was the average of six repeated scans (step resolution 1 nm, 1 s each step) from which the corresponding background spectrum was subtracted. Quantitative prediction of the helical content was accomplished by fitting CD data with the Hennessey-Johnson algorithm (26), by the program CDNN in "simple spectra" configuration (27), using a protein data base with known secondary structure as the basis set.

**Liposome Turbidity Assay**—Liposomes composed of EPC and CHOL (molar ratio of 2:1) and with increasing amounts of PEG2000-DSPE (0, 2.5, 5, and 10 mol %) were added to a cuvette at a concentration of 300 or 1000  $\mu$ M in a final volume of 1.5 ml of HBS. Immediately after the addition of diINF-7 (lipid/peptide molar ratio of 50), peptide-induced aggregation of liposomes at the indicated pH values was determined by measuring the increase in optical density of the liposome dispersion with a spectrophotometer at 500 nm over a period of 8–12 min at room temperature.

**Liposome Leakage Assay**—A serial dilution (1:5) of free or liposome-encapsulated diINF-7 peptide was prepared in a 96-well microtiter plate by transferring 20  $\mu$ l of the initial peptide solution (50  $\mu$ g/ml for free peptide and 0.3  $\mu$ g/ml for liposome-entrapped peptide) from one well to the next well containing 80  $\mu$ l of HBS. Calcein-containing liposomes were added to each well at a final concentration of 40  $\mu$ M. After a 60-min incubation at room temperature, samples were analyzed for fluorescence with an LS50B fluorimeter (PerkinElmer Life Sciences) set at an excitation wavelength of 488 nm and an emission wavelength of 520 nm. Calcein leakage was expressed relative to the difference in the fluorescence of calcein liposomes incubated in the absence of diINF-7 peptide (0% leakage) and the fluorescence of calcein liposomes that had been disrupted with 0.5% (v/v) Triton X-100 (100% leakage). The effect of Triton X-100 on calcein fluorescence intensity was negligible at the tested concentration (28, 29).

**Lipid Mixing Assay**—diINF-7-induced lipid mixing was monitored with the pyrene excimer assay developed by Galla and Hartmann (30). Liposomes (5  $\mu$ M) labeled with 10 mol % PyrPC (Molecular Probes, Inc., Eugene, OR) were mixed in a total volume of 1.4 ml of HBS with a 20-fold molar excess of nonlabeled donor liposomes in a cuvette kept at 37 °C. diINF-7 peptide was added at the amounts indicated, and after a 2-min equilibration period, the pH of the medium in the cuvette was lowered to 5.2 by adding one-twentieth volume of fusion buffer (0.1 M Mes, 0.1 M acetic acid, pH 4.1). Fusion was continuously monitored at 37 °C by measuring the decrease in PyrPC excimer fluorescence with an LS50B fluorimeter set at an excitation wavelength of 345 nm and an emission wavelength of 480 nm while the cuvette contents were continuously stirred. The decrease of fluorescence was expressed relative to the difference in the initial fluorescence and the excimer fluorescence at infinite dilution, which was obtained by disrupting the liposomes with 0.5% (v/v) Triton X-100 (final concentration).

**Aqueous Contents Mixing Assay**—The occurrence of diINF-7-induced intermixing of liposome-entrapped solutes was determined with a fluorescent assay based on quenching of calcein with bivalent metal ions (31). Unilamellar liposomes of 150 nm in size containing calcein (0.8 mM) and  $\text{CuSO}_4$  (1 mM) in HBS were admixed at a concentration of 50

TABLE I  
Amino acid sequences of fusion peptides

INF HA-2, amino-terminal sequence of Influenza virus X-31 (H3N2) hemagglutinin subunit HA-2; diINF-7, peptide analogue resembling Inf HA-2 dimerized at the COOH terminus by disulfide bond formation between COOH-terminal cysteine residues. Differences in amino acid sequence of diINF-7 compared with the native Inf HA-2 sequence are highlighted in boldface type.

Peptide	Sequence					
Inf HA-2	GLF	GAI	AGFI	ENGW	EGMI	DGWYG-----
diINF-7	GLF	<b>EAI</b>	<b>EGFI</b>	ENGW	EGMI	DGWYGC
	GLF	<b>EAI</b>	<b>EGFI</b>	ENGW	EGMI	DGWYGC

$\mu$ M with a 5-fold molar excess of liposomes containing 20 mM EDTA in a stirred cuvette kept at a temperature of 37 °C. diINF-7 was added at a concentration of 5  $\mu$ g/ml. The pH of the buffer was lowered to 5.2 by adding one-twentieth volume of fusion buffer. Aqueous contents mixing and/or leakage were continuously monitored at 37 °C by measuring the increase in calcein fluorescence with a fluorimeter set at an excitation wavelength of 488 nm and an emission wavelength of 520 nm. To be able to determine the contribution of both leakage and aqueous content mixing to the total increase in calcein fluorescence, one-twentieth volume of 1 mM  $\text{CuSO}_4$  was added to the external medium during the fusion process.

**Cytotoxicity Assay**—OVCAR-3 cells were plated in 96-well cell culture plates at  $5 \times 10^3$  cells/well and cultured for 24 h. Culture medium was removed by decanting the plates, and cells were overlaid with 100  $\mu$ l of fresh culture medium. To the first well of each column 100  $\mu$ l of liposome formulation was added at a final lipid concentration of 1 mM (corresponding to 0.5  $\mu$ g/ml of DTA). 2-Fold serial dilutions of liposome formulations were prepared by transferring 100  $\mu$ l of the first well in a column to the next and so forth. After a 1-h incubation at 37 °C, liposomes were removed from the cells by decanting the plates, and cells were washed with 100  $\mu$ l/well of fresh culture medium and overlaid with 100  $\mu$ l of fresh culture medium before incubation was continued. Forty-eight hours after the addition of liposome formulations, cell viability was assessed with the colorimetric XTT assay as previously described (32).

## RESULTS

**Primary and Secondary Structure of diINF-7**—The primary amino acid sequence of diINF-7 is presented in Table I. Compared with the native sequence of the  $\text{NH}_2$ -terminal domain of the influenza virus HA-2 subunit, diINF-7 differs in only two amino acids; glycine at position 4 and alanine at position 7 have been substituted by glutamic acid residues. These substitutions favor the pH dependence of the fusogenic activity of the peptide. Since fusogenic activity is thought to be directly correlated with  $\alpha$ -helix formation of the peptide (6, 33–35), the secondary structure of diINF-7 was determined by circular dichroism spectropolarimetry at both pH 7.4 and pH 5.2 in the presence or absence of detergent-solubilized phospholipids. Since Subbarao *et al.* (36) showed that interpretation of CD spectra below 222 nm in the presence of phospholipid vesicles is ambiguous due to liposome scattering, we used mixed micelles of phospholipids and detergent to determine the effect of a hydrophobic environment on the helical content of the peptide. The CD spectrum (Fig. 1) of the free peptide at pH 5.2 shows minima at 208 and 222 nm, typical of a highly  $\alpha$ -helical structure; in contrast, at neutral pH, the diINF-7 peptide is primarily randomly coiled (Fig. 1A and Table II). Interestingly, the presence of detergent-solubilized phospholipids can also induce  $\alpha$ -helix formation of diINF-7 (Fig. 1B and Table II).

**Liposome Characterization**—In this study, neutral liposomes (EPC/CHOL molar ratio 2:1) with and without incorporated PEG2000-DSPE were used as model membranes to test the membrane-destabilizing capacity of diINF-7 and targeted drug carriers to deliver DTA into the cytosol of tumor cells. Liposomes were prepared by hydrating lipid films of 30  $\mu$ mol of total lipid with 1 ml of the appropriate buffer, after which the formed liposomes were sized by extrusion (37). The lipid com-

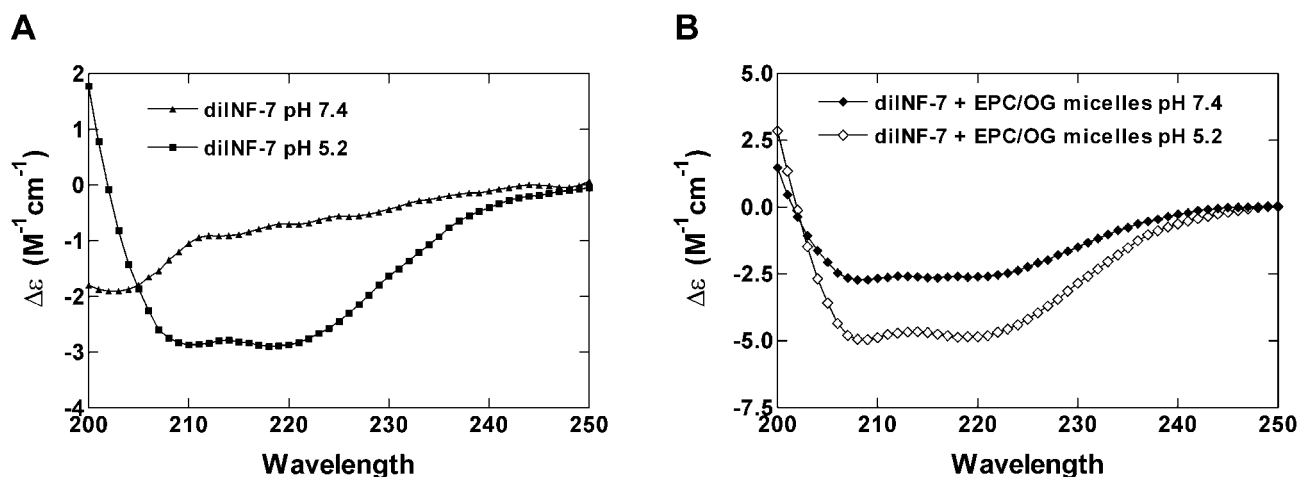


FIG. 1. Secondary structure of diINF-7 peptides as a function of pH and presence of mixed micelles of phospholipids and detergent. CD spectra of diINF-7 at pH 5.2 and 7.4 in the absence (A) and presence (B) of phospholipid micelles against appropriate blanks at 25 °C are shown. In all cases, the concentration of diINF-7 peptide was 18.6  $\mu\text{M}$ . Mixed micelles consisted of 1 mM indicated phospholipids and 40 mM octyl glucoside (OG). As judged from the ellipticity at 222 nm,  $\alpha$  helicity of diINF-7 peptides increased with decreasing pH and in the presence of detergent or mixed micelles.

TABLE II  
Molar absorbance difference at 222 nm ( $\Delta\epsilon_{222}$ ) and helical content of diINF-7 in the absence or presence of mixed micelles and at different pH values

Mixed micelles	pH	$\Delta\epsilon_{222}$	Helical content
		$\text{M}^{-1}\text{cm}^{-1}$	%
	7.4	-0.675	15
	5.2	-2.751	31
EPC/OG (1 mM/40 mM)	7.4	-2.538	29
EPC/OG (1 mM/40 mM)	5.2	-4.686	53

TABLE III  
Characterization of liposome preparations used throughout this study

Liposome composition (molar ratio)	Lipid concentration	Entrapped contents	Average size (polydispersity)
	mM PL		nm
EPC/CHOL (2:1)	8.2		90 (0.110)
EPC/CHOL (2:1)	8.8		150 (0.101)
EPC/CHOL (2:1)	7.6		270 (0.326)
EPC/CHOL (2:1)	7.1		748 (0.555)
EPC/CHOL (2:1)	6.2	diINF-7 (12 $\mu\text{g}/\mu\text{mol}$ PL)	194 (0.397)
EPC/CHOL (2:1)	10.3	DTA (0.5 $\mu\text{g}/\mu\text{mol}$ PL)	152 (0.123)
EPC/CHOL (2:1)	7.7	DTA/diINF-7 (12 $\mu\text{g}$ total protein/ $\mu\text{mol}$ PL)	193 (0.405)
EPC/CHOL (2:1)	8.0	Calcein (90 mM)	130 (0.096)
EPC/CHOL (2:1)	6.8	Calcein (90 mM)/diINF-7 (10 $\mu\text{g}/\mu\text{mol}$ PL)	188 (0.368)
EPC/CHOL/PEG2000-DSPE (1.95:1:0.05)	6.2		127 (0.091)
EPC/CHOL/PEG2000-DSPE (1.9:1:0.1)	7.1		128 (0.084)
EPC/CHOL/PEG2000-DSPE (1.8:1:0.2)	7.4		127 (0.021)

position, phospholipid concentration, entrapped contents, and liposome size of the batches of liposomes used throughout this study are given in Table III.

**diINF-7 Peptide-induced Aggregation of Liposomes**—diINF-7 peptide-induced aggregation of liposomes as a function of pH and the presence of PEG molecules on the surface of liposomes was monitored by measuring the changes in turbidity of liposome dispersions at 500 nm (Fig. 2). The results show that liposome aggregation increased with decreasing pH. No aggregation of liposomes was observed at pH 8.4. The presence of PEG molecules ( $M_r$  2000) exposed on the surface of liposomes (2.5, 5, and 10 mol % relative to total lipid) fully inhibited diINF-7-induced liposome aggregation at low pH.

**Lipid Mixing Assay**—The capacity of diINF-7 to induce membrane fusion between liposomes was determined with the pyrene excimer lipid-mixing assay (30). “Donor” liposomes, containing 10 mol % of PyrPC were admixed with nonlabeled “acceptor” liposomes. Upon intermixing of membrane lipids

between donor and acceptor liposomes, the PyrPC label will be diluted over a larger membrane area, resulting in a decrease in excimer formation and thus a decrease in PyrPC fluorescence. Fig. 3 shows that the extent of lipid mixing increased with increasing concentrations of diINF-7. Lipid mixing was pH-dependent. No lipid mixing was observed at pH 7.4. In an acidic environment, the rate and extent of lipid mixing increased with increasing diINF-7 concentration (Fig. 3A) and decreasing pH (Fig. 3B). Furthermore, the degree of lipid mixing depended on the size of acceptor and donor liposomes (Fig. 3C). Small liposomes with an average size of 70 nm showed the highest degree of lipid mixing (75%), whereas the extent of lipid mixing between liposomes with an average size of  $\sim$ 700 nm was only 22%. Furthermore, the extent of lipid mixing was negatively correlated with the amount of PEG2000 exposed on the surface of liposomes (Fig. 3D).

**diINF-7-mediated Membrane Destabilization Results in Leaky Membrane Fusion**—A fluorescent assay based on the

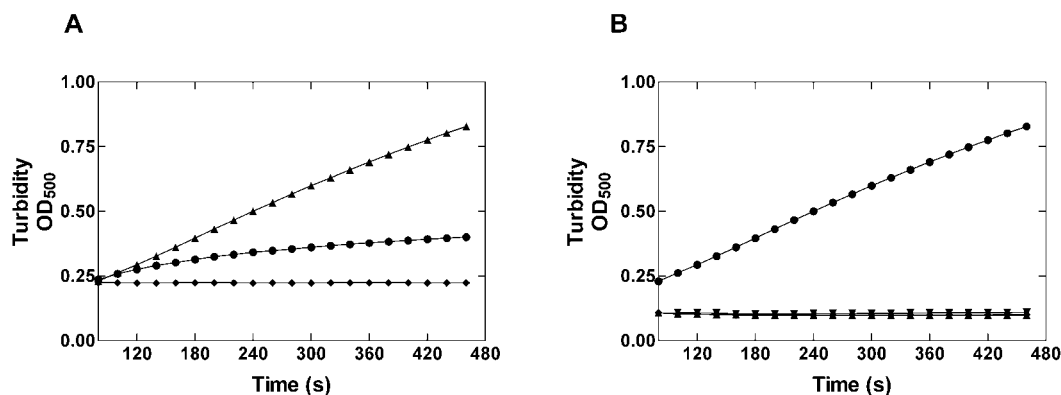


FIG. 2. diINF-7 peptide-induced aggregation of liposomes as a function of pH and liposome composition. A, aggregation of liposomes ( $300 \mu\text{M}$ ) when exposed to diINF-7 peptides dissolved in the aqueous dispersion (lipid/peptide molar ratio 50) at pH 5.2 ( $\blacktriangle$ ), 7.4 ( $\bullet$ ), and 8.4 ( $\blacklozenge$ ). B, effect of PEG2000 exposed to the surface of liposomes on diINF-7 induced aggregation of liposomes at pH 5.2. Liposomes contained 0 mol % ( $\bullet$ ), 2.5 mol % ( $\blacktriangledown$ ), 5 mol % ( $\blacklozenge$ ), and 10 mol % ( $\blacktriangle$ ) of PEG2000-DSPE relative to the total amount of lipid. Concentrations of liposomes and peptide were the same as in A.

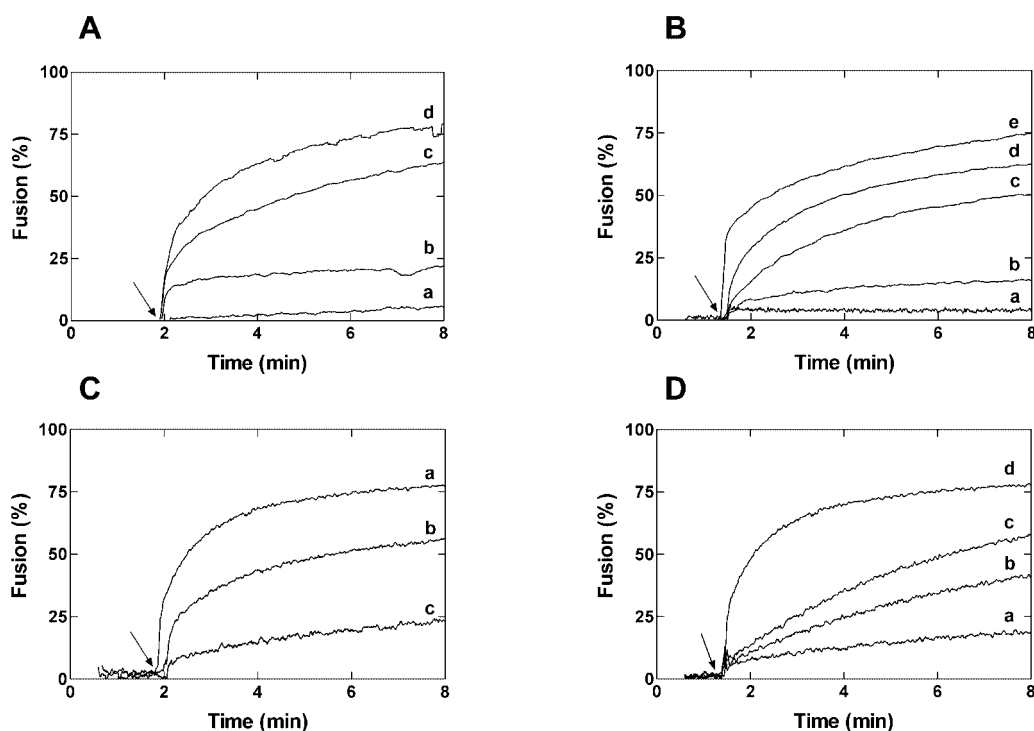
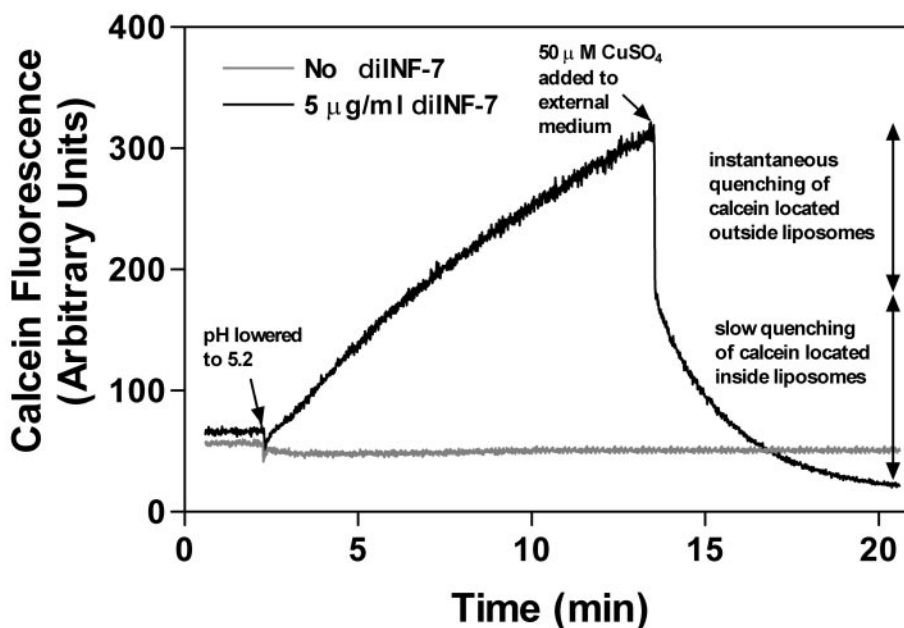


FIG. 3. Effect of diINF-7 peptide concentration, buffer pH, liposome size, and surface-exposed PEG molecules on the extent of diINF-7-induced lipid mixing. Donor liposomes (EPC/CHOL/PyrPC, molar ratio 1.8:1:0.2) were admixed with a 20-fold molar excess of acceptor liposomes (EPC/CHOL, molar ratio 2:1) at a final lipid concentration of  $105 \mu\text{M}$ . diINF-7 peptides were added to the liposome dispersion at the indicated concentration. At the time point indicated with a black arrow, the external medium was acidified to pH 5.2 (unless mentioned otherwise), and lipid mixing was continuously monitored as measured by a decrease of PyrPC excimer fluorescence. The decrease of PyrPC excimer fluorescence was expressed relative to the initial fluorescence and the excimer fluorescence at infinite dilution (*i.e.* after vesicle solubilization with detergent). A, extent of lipid mixing as a function of diINF-7 peptide concentration: 0 (a), 1 (b), 10 (c), and 20 (d)  $\mu\text{g/ml}$  diINF-7. B, influence of pH on degree of lipid mixing induced by diINF-7 (10  $\mu\text{g/ml}$ ): pH 7.4 (a), 6.5 (b), 5.2 (c), 5.0 (d), and 4.6 (e). C, influence of liposome size on the degree of lipid mixing induced by diINF-7 (10  $\mu\text{g/ml}$ ). Curves show lipid mixing between liposomes of 90 nm (a), 270 nm (b), and 750 nm (c) in size. D, effect of surface-exposed PEG molecules on the degree of diINF-7-induced lipid mixing between 100-nm liposomes. Peptide concentration was 10  $\mu\text{g/ml}$ . The relative amount of PEG2000 molecules grafted on the surface of liposomes was 10 mol % (a), 5 mol % (b), 2.5 mol % (c), and 0 mol % (d). Each curve represents the average of three individual measurements.

method of Kendall and MacDonald (31) to monitor vesicle fusion and lysis was performed to determine whether diINF-7-induced lipid mixing is accompanied by intermixing of aqueous contents between liposomes and/or leakage of liposome-entrapped materials. Calcein- $\text{Cu}^{2+}$  complexes, which are nonfluorescent, were entrapped in one set of liposomes and admixed with a 5-fold excess of a second set of liposomes containing entrapped EDTA. When EDTA comes in contact with  $\text{Cu}^{2+}$ -calcein complexes, either due to aqueous contents mixing between liposomes or due to leakage of both compounds to the

external medium, EDTA will chelate the  $\text{Cu}^{2+}$  ions, thereby liberating the highly fluorescent calcein. The results of diINF-7-induced aqueous contents mixing between EDTA-containing liposomes and  $\text{Cu}^{2+}$ -calcein-containing liposomes are presented in Fig. 4. An increase in calcein fluorescence was observed directly after lowering the pH of the external medium to 5.2. To be able to discriminate which part of the observed increase in calcein fluorescence was caused by leakage of entrapped calcein and EDTA and which part was caused by intermixing of aqueous contents, an excess of  $\text{Cu}^{2+}$  ions was

FIG. 4. **diINF-7-induced aqueous contents mixing and leakage of liposomes.** Liposomes ( $50 \mu\text{M}$  of total lipid) containing  $1 \text{ mM}$   $\text{CuSO}_4$  and  $0.8 \text{ mM}$  calcein were admixed with a 5-fold excess of liposomes containing  $20 \text{ mM}$  EDTA. Fluorescence of calcein was continuously monitored with an LS50B fluorescent spectrophotometer set at excitation wavelength of  $488 \text{ nm}$  and an emission wavelength of  $520 \text{ nm}$ . At the indicated time points, the pH of the external medium was lowered from  $7.4$  to  $5.2$ , and one-twentieth volume of  $1 \text{ mM}$   $\text{CuSO}_4$  was added to the external medium. *Black curve*, calcein fluorescence pattern obtained in the presence of  $5 \mu\text{g/ml}$  diINF-7. *Gray curve*, calcein fluorescence pattern obtained in the absence of diINF-7 peptide. Results of a typical experiment are shown.



added to the external medium. This resulted in an instantaneous decrease in calcein fluorescence, followed by a slow decline in calcein fluorescence. This biphasic decrease of calcein upon the addition of  $\text{Cu}^{2+}$  ions to the external medium may be explained by instantaneous quenching of calcein located outside liposomes, whereas quenching of free calcein located inside lipidic vesicles occurred at a slower rate, since this requires passage of  $\text{Cu}^{2+}$  ions over the diINF-7 peptide-destabilized liposome membranes. No increase in calcein fluorescence could be observed in the absence of diINF-7 peptides.

**Effect of Liposome Encapsulation on the Membrane Destabilizing Capacity of diINF-7**—Previous studies with synthetic analogues of influenza virus fusion peptides have demonstrated that peptide-induced membrane destabilization is accompanied by leakage of liposome-entrapped materials when peptides were added in free form to the liposomes (17, 20, 38, 39). Here, we tested the capacity of diINF-7 to induce leakage of calcein from liposomes under two different conditions: 1) by adding diINF-7 peptide free in solution to a dispersion of calcein-containing liposomes or 2) by adding liposome-entrapped diINF-7 to calcein-containing liposomes. Fig. 5A presents the results of calcein leakage from liposomes composed of EPC and CHOL (molar ratio 2:1) after 1 h of incubation at room temperature in the presence of increasing diINF-7 peptide concentrations. Calcein leakage occurred both at pH 5.2 and pH 7.4. However, at pH 7.4, 30-fold higher concentrations of diINF-7 were needed to obtain the same level of calcein leakage. diINF-7 also induced leakage of calcein from liposomes at pH 5.2 when encapsulated in liposomes other than the calcein-liposomes although less efficiently than free diINF-7 (Fig. 5B).

**Effect of Liposome-encapsulated diINF-7 on Cytosolic DTA Delivery**—An important finding in this study is that diINF-7 induced leakage of calcein from liposomes upon exposure to low pH when these peptides were encapsulated in liposomes other than the calcein-containing liposomes. This finding implies that diINF-7 peptides may be able to destabilize not only the carrier liposomes in which these peptides are entrapped but also the endosomal membranes when these fusion peptide-bearing liposomes are endocytosed by target cells. To evaluate the endosomolytic activity of diINF-7, we co-encapsulated DTA in diINF-7-containing liposomes. DTA/diINF-7 liposomes were targeted to the internalizing human EGFR by conjugating mAb

425 to the liposome surface. These immunoliposomes were incubated with ovarian carcinoma cells (OVCAR-3) expressing the EGFR on their cell surface. Binding of DTA/diINF-7 liposomes labeled with the fluorescent probe DiD is illustrated in Fig. 6A, which shows that the immunoliposomes are able to bind to OVCAR-3 cells. Cell binding could be partially blocked by adding free mAb 425 at a concentration of  $500 \mu\text{g/ml}$ . Liposomes lacking surface-grafted antibodies showed only low levels of cell binding, and liposomes bearing an isotype-matched irrelevant antibody (mAb 12CA5 directed against influenza virus HA) grafted on their surface showed moderate binding. Confocal laser-scanning microscopy experiments show that liposomes targeted to the EGFR on OVCAR-3 cells are efficiently internalized (Fig. 6B).

Cytotoxicity of native DT, free DTA, and liposomal DTA formulations toward OVCAR-3 cells is shown in Fig. 7. DTA in free form was not toxic to OVCAR-3 cells in the concentration range tested, whereas the nicked DT showed concentration-dependent cytotoxicity toward OVCAR-3 cells (Fig. 7A). Importantly, the cytotoxicity of diINF-7/DTA-containing immunoliposomes (DTA-425-FIL) was even higher compared with native DT, indicating that the amount of toxin molecules delivered by immunoliposomes via EGFR-mediated endocytosis and subsequent endosomal escape is higher than the amount of toxin delivered via the native HB-EGF receptor (Fig. 7, B and C). DTA-immunoliposome formulations devoid of diINF-7 (DTA-425-IL) did not show cytotoxicity. Cytotoxicity was not due to diINF-7-induced endosomal membrane disruption, since immunoliposomes bearing diINF-7 but no DTA (425-FIL) did not show toxicity toward OVCAR-3 cells (Fig. 7C). diINF-7/DTA-liposomes that were nontargeted or targeted with an irrelevant monoclonal antibody did not show cytotoxicity (Fig. 7B). Inhibition of acidification of endosomes by adding  $20 \text{ mM}$   $\text{NH}_4\text{Cl}$  to the culture medium 30 min prior to adding the diINF-7/DTA immunoliposomes resulted in loss of cytotoxicity of this DTA formulation (Fig. 7B). The addition of  $20 \text{ mM}$   $\text{NH}_4\text{Cl}$  to the culture medium had no effect on cell viability (results not shown). In conclusion, the results show that cytosolic delivery of DTA into OVCAR-3 cells requires both receptor-mediated endocytosis of DTA/diINF-7 immunoliposomes and subsequent low pH-induced activation of the endosomolytic activity of diINF-7.

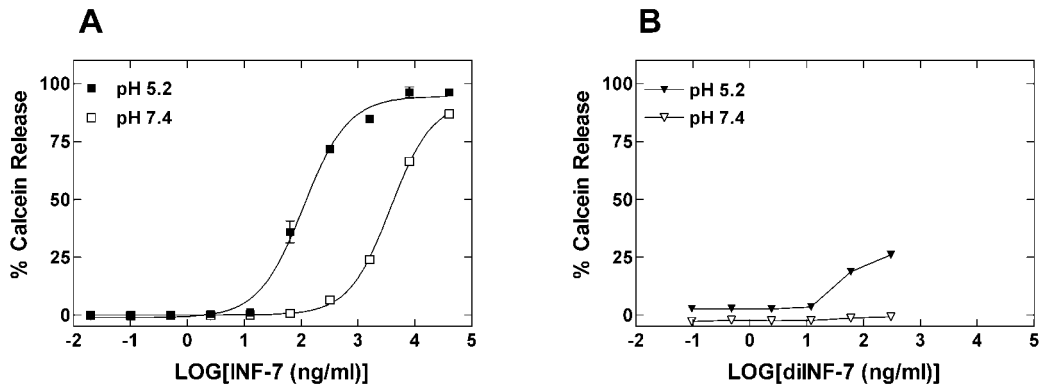


FIG. 5. Effect of liposome-encapsulated diINF-7 peptide compared with free diINF-7 peptide on the extent of calcein leakage from liposomes at pH 5.2 and pH 7.4. Shown is leakage of calcein from liposomes composed of EPC and CHOL (molar ratio 2:1) and approximately 130 nm in size induced by diINF-7 peptides free in solution (A) and diINF-7 peptides encapsulated in liposomes other than the liposomes containing the calcein (B). Leakage of calcein from liposomes was measured both at pH 7.4 and pH 5.2 after 1-h incubation at room temperature. Leakage of calcein is expressed relative to the difference between leakage of calcein from liposomes after disruption with detergent (100% value) and leakage of calcein from liposomes in the absence of peptides (0% value). Each data point represents the average of three individual measurements.

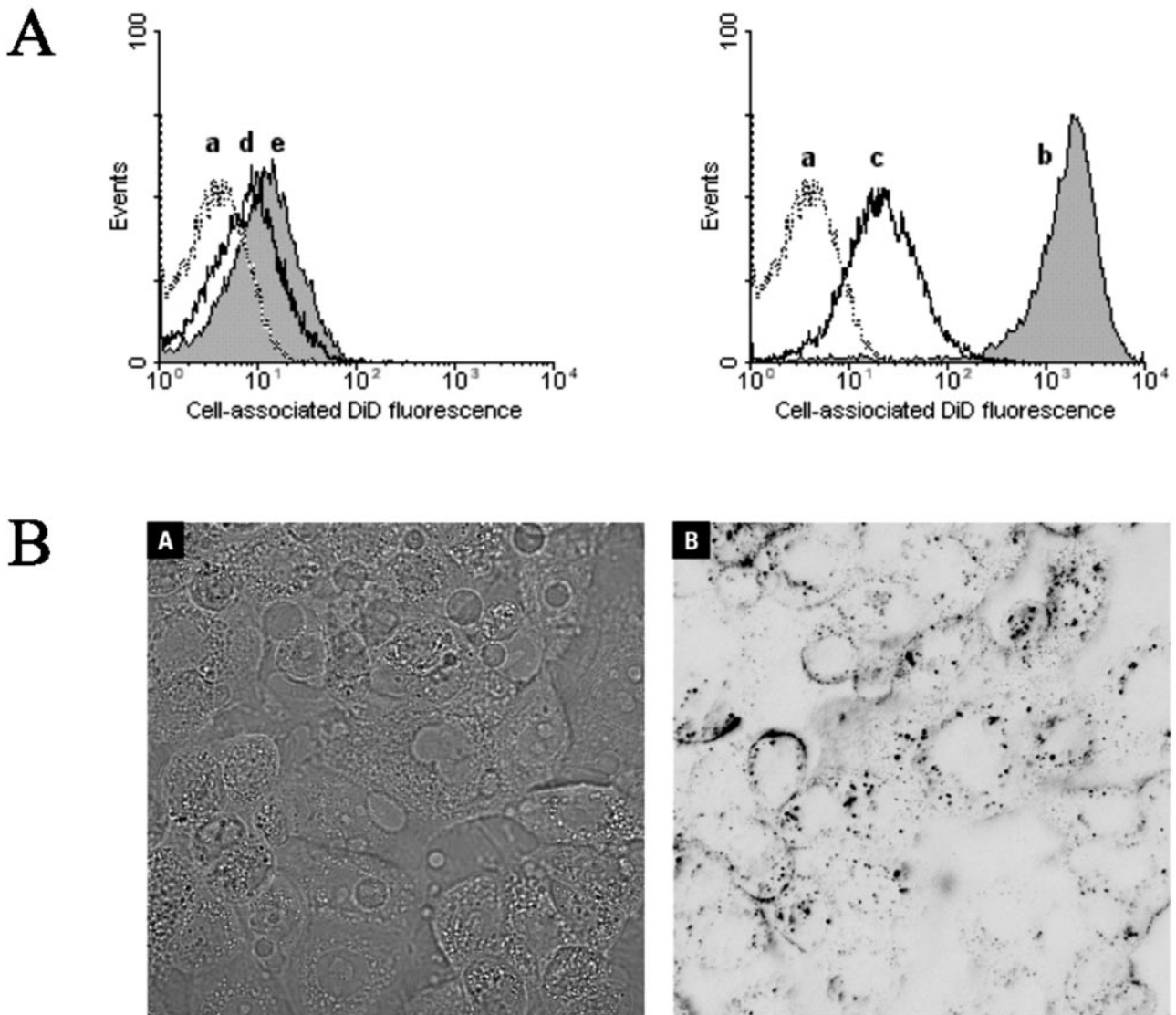
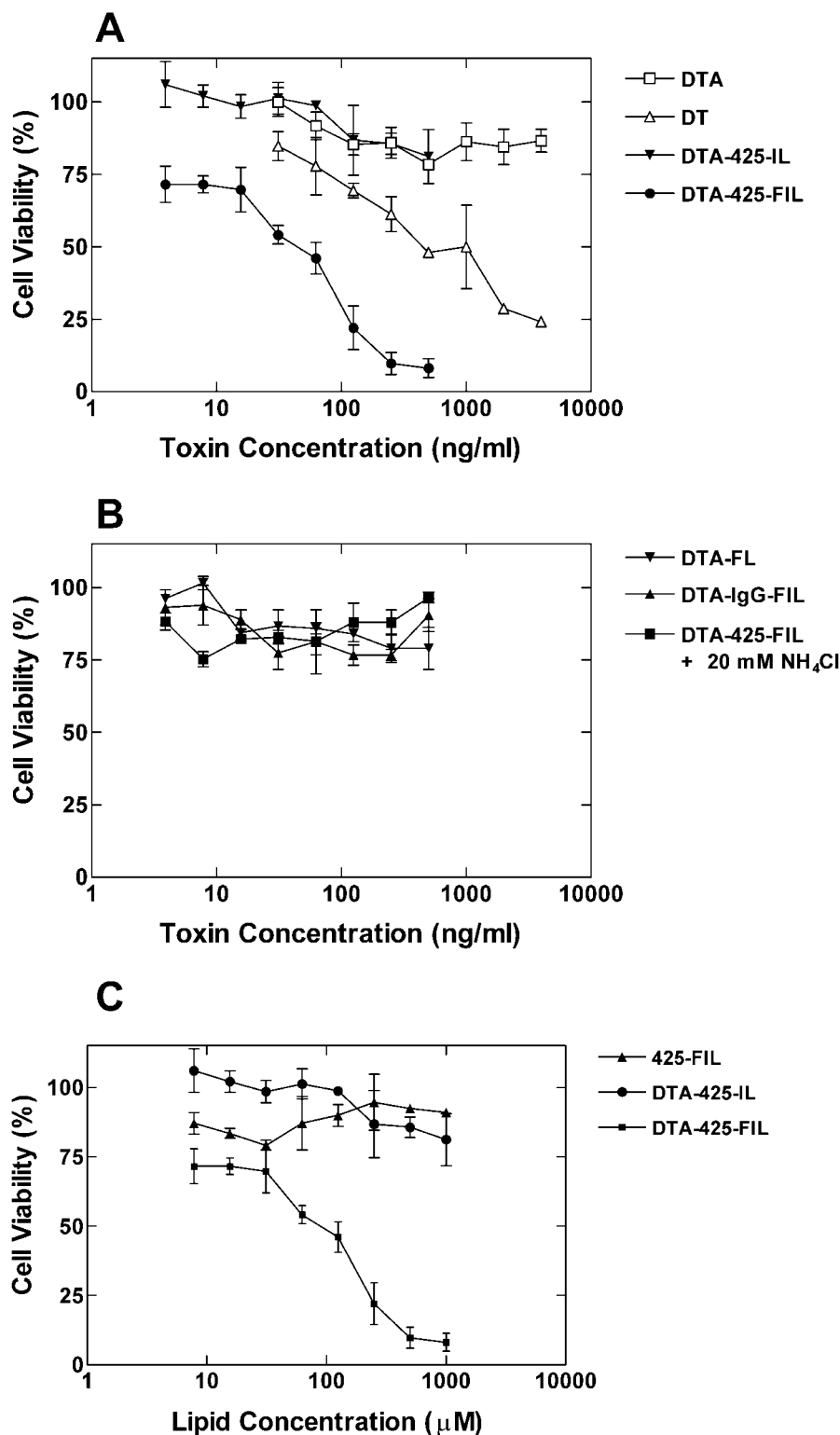


FIG. 6. Flow cytometry (A) and confocal laser scanning microscopy (CLSM; B) analysis of cellular uptake of diINF-7/DTA-containing immunoliposomes by OVCAR-3 cells. Cells ( $2 \times 10^5$ ) were incubated with DiD-labeled liposomes (EPC/CHOL/DiD, 2:1:0.002) or immunoliposomes ( $500 \mu\text{M}$ ) for 1 h at  $37^\circ\text{C}$ . Liposomes contained  $0.5 \mu\text{g}/\mu\text{mol}$  PL of DTA and  $12 \mu\text{g}/\mu\text{mol}$  PL of diINF-7. After unbound liposomes were washed away, cells were analyzed for associated DiD fluorescence by flow cytometry. A, cell-associated DiD fluorescence of OVCAR-3 cells incubated without liposomes (a), with 425-IL (b), with 425-IL in the presence of free mAb 425 ( $500 \mu\text{g}/\text{ml}$ ) (c), liposomes without surface-conjugated antibodies (d), and immunoliposomes bearing isotype-matched irrelevant mAb 12CA5 (e). B, light contrast (A) and CLSM (B) pictures taken from OVCAR-3 cells incubated for 60 min with 425-IL with encapsulated DTA and diINF-7.



**FIG. 7. Cytotoxicity of free or liposome-encapsulated DTA toward OVCAR-3 cells.** OVCAR-3 cells, plated at a density of  $5 \times 10^4$  cells/ml were exposed to several DT or DTA formulations for 1 h at 37 °C. Thereafter, toxin formulations were removed, and cells were incubated for 47 h before cell viability was assessed with the XTT assay. Cell viability is expressed relative to the difference in viability of untreated cells (100% value) and empty wells (0% viability). **A**, DT, crude diphtheria toxin activated with trypsin; *DTA-425-IL*, immunoliposomes targeted with an anti-EGFR antibody (mAb 425) and containing DTA ( $0.5 \mu\text{g}/\mu\text{mol}$  PL); *DTA-425-FIL*, 425-IL containing DTA ( $0.5 \mu\text{g}/\mu\text{mol}$  PL) and diINF-7 ( $12 \mu\text{g}/\mu\text{mol}$  PL). **B**, *DTA-FL*, nontargeted liposomes containing DTA ( $0.5 \mu\text{g}/\mu\text{mol}$  PL) and diINF-7 ( $12 \mu\text{g}/\mu\text{mol}$  PL); *DTA-IgG-FIL*, immunoliposomes targeted with an isotype-matched irrelevant antibody and containing DTA ( $0.5 \mu\text{g}/\mu\text{mol}$  PL) and diINF-7 ( $12 \mu\text{g}/\mu\text{mol}$  PL); *DTA-425-FIL + 20 mM NH<sub>4</sub>Cl*, *DTA-425-FIL* incubated with OVCAR-3 cells in the presence of 20 mM NH<sub>4</sub>Cl to inhibit endosome acidification. **C**, *425-FIL*, 425-IL containing diINF-7 ( $12 \mu\text{g}/\mu\text{mol}$  PL).

#### DISCUSSION

In the work presented here, a dimerized synthetic fusion peptide (diINF-7) resembling the NH<sub>2</sub>-terminal domain of influenza virus hemagglutinin subunit HA-2 was used for the purpose of enhancing cytosolic delivery of immunoliposome-encapsulated macromolecules after cellular uptake of immunoliposomes by receptor-mediated endocytosis. Structural characterization of diINF-7 showed that the dimeric peptide adopts an  $\alpha$ -helix when exposed to low pH and when exposed to mixed micelles of detergent and phospholipids. The pH-dependent

membrane destabilizing capacity of diINF-7 was demonstrated by the induction of leakage of calcein from liposomes. An important finding for the application of diINF-7 as an endosomal agent in liposomal drug delivery is that, although less effective than free diINF-7 peptide, liposome-encapsulated diINF-7 peptides are able to induce release of calcein from another set of liposomes when the pH of the external medium is lowered (Fig. 5). This indicates that the liposome-encapsulated peptides are not only able to destabilize the liposomes in which they are encapsulated but, subsequently, also other lipid mem-

branes. Activation of the membrane fusion capacity of liposome-encapsulated diINF-7 peptides requires exposure to low pH. The internal pH within the liposomes will be the same as the pH of the buffer in which the lipid films were hydrated (in this case HBS, pH 7.4). When liposomes are exposed to a lower external pH, it is expected that the pH inside the liposomes will slowly drop in time as protons and hydroxyl ions cross the liposome bilayer fairly quickly, probably as a result of transfer of hydrogen bonds between water molecules (40, 41). Therefore, it is likely that liposome-encapsulated diINF-7 peptides will slowly become activated due to the decline of the pH within the liposomes. Moreover, the presence of diINF-7 peptides associated with the liposome bilayer may further increase the permeability of the bilayer to protons. The observation of a relatively small degree of calcein release induced by liposome-entrapped diINF-7 peptides compared with free diINF-7 peptides is indicative of such a slow decrease in internal pH and a concomitant slow activation of the entrapped fusion peptides.

Besides leakage, the diINF-7 peptide also induces liposome aggregation (Fig. 2) and subsequent intermixing of lipids between liposome vesicles, indicative of membrane fusion (Fig. 3). The degree of lipid mixing induced by diINF-7 seemed to be dependent on the size of liposomes. An explanation for this may be that small liposomes have a high curvature and membrane strain, which favors merging with other vesicles to release the strain. Conversely, multilamellarity of large liposomes may account for the decrease in observed lipid mixing. An interesting observation is that incorporation of only small amounts of PEG-lipids in the liposome membranes (2.5 mol %) completely inhibited liposome aggregation and caused a large reduction in lipid mixing (Figs. 2B and 3D). Presumably, the hydrophilic PEG polymers prevented the close juxtaposition of membranes required for peptide-induced aggregation of liposomes and subsequent membrane exchange between aggregated liposomes. diINF-7 peptide-induced fusion is a rather leaky process, resulting in excessive leakage of liposome-entrapped compounds to the external medium in addition to mixing of aqueous contents between fused liposomes (Fig. 4). Similar findings have been reported for fusion induced by intact influenza virus particles with liposomes (42).

In a second set of experiments, diINF-7 was tested on its capacity to enhance endosomal escape of immunoliposome-entrapped compounds. diINF-7 together with DTA were entrapped inside immunoliposomes targeted to the EGFR expressed on the surface of OVCAR-3 cells. We have utilized encapsulation of diINF-7 as a means to guarantee delivery of sufficient quantities of peptides into the endosomal compartment, which is required for effective destabilization of liposomal as well as endosomal membranes with subsequent cytosolic drug release. The possibility to attach the fusogenic peptide to the liposome membrane has been explored by us<sup>2</sup> and several other groups (38, 43–45). However, the general conclusion is that lipid modification of fusogenic peptides leads to an altered conformation of the peptides, thereby influencing their fusogenic behavior (38, 45). The results presented in this study demonstrate that co-encapsulation of diINF-7 into DTA-containing immunoliposomes results in cytosolic delivery of DTA into OVCAR-3 cells. As inhibition of endosome acidification results in loss of cytotoxicity of diINF-7/DTA-containing immunoliposomes, it is most likely that delivery of DTA into the cytosol of OVCAR-3 cells is mediated by diINF-7-induced endosomal membrane destabilization after cellular uptake of the diINF-7/DTA immunoliposomes.

In conclusion, encapsulation of the fusogenic peptide diINF-7 into immunoliposomes is an attractive strategy to obtain endosomal escape of liposome-entrapped proteins after receptor-mediated endocytosis of these immunoliposomes by target cells. These immunoliposomes will be a valuable tool for cytosolic delivery of membrane-impermeable proteins or nucleic acids to specific cells for experimental, diagnostic, or therapeutic purposes.

*Acknowledgments*—We thank Lovina Hofmeyer (Department of Medicinal Chemistry, Utrecht Institute for Pharmaceutical Sciences, Utrecht University, The Netherlands) for INF-7 peptide synthesis.

## REFERENCES

- Scheule, R. K. (1986) *Biochemistry* **25**, 4223–4232
- Stegmann, T., Morselt, H. W., Booy, F. P., van Breemen, J. F., Scherphof, G., and Wilschut, J. (1987) *EMBO J.* **6**, 2651–2659
- Schoen, P., Chonn, A., Cullis, P. R., Wilschut, J., and Scherrer, P. (1999) *Gene Ther.* **6**, 823–832
- Kaneda, Y. (2000) *Adv. Drug. Del. Rev.* **43**, 197–205
- Plank, C., Zauner, W., and Wagner, E. (1998) *Adv. Drug. Del. Rev.* **34**, 21–35
- Pecheur, E. I., Sainte-Marie, J., Bienven, and Hoekstra, D. (1999) *J. Membr. Biol.* **167**, 1–17
- Fujii, G. (1999) *Adv. Drug. Del. Rev.* **38**, 257–277
- Wagner, E. (1999) *Adv. Drug. Del. Rev.* **38**, 279–289
- Mechtler, K., and Wagner, E. (1997) *New J. Chem.* **21**, 105–111
- Oberhauser, B., Plank, C., and Wagner, E. (1995) in *Delivery Strategies for Antisense Oligonucleotide Therapeutics* (Akhtar, S., ed) CRC Press, Inc., Boca Raton, FL
- Han, X., Bushweller, J. H., Cafiso, D. S., and Tamm, L. K. (2001) *Nat. Struct. Biol.* **8**, 715–720
- Matsumoto, T. (1999) *Biophys. Chem.* **79**, 153–162
- Düzgünes, N., and Shavnin, S. A. (1992) *J. Membr. Biol.* **128**, 71–80
- Pichon, C., Freulon, I., Midoux, P., Mayer, R., Monsigny, M., and Roche, A. C. (1997) *Antisense Nucleic Acid Drug Dev.* **7**, 335–343
- Freulon, I., Roche, A. C., Monsigny, M., and Mayer, R. (2001) *Biochem. J.* **354**, 671–679
- Kichler, A., Mechtler, K., Behr, J. P., and Wagner, E. (1997) *Bioconj. Chem.* **8**, 213–221
- Wagner, E., Plank, C., Zatloukal, K., Cotten, M., and Birnstiel, M. L. (1992) *Proc. Natl. Acad. Sci. U. S. A.* **89**, 7934–7938
- Baru, M., Nahum, O., Jaaro, H., Sha'anani, J., and Nur, I. (1998) *J. Drug Target.* **6**, 191–199
- Hamilton, T. C., Young, R. C., McKoy, W. M., Grotzinger, K. R., Green, J. A., Chu, E. W., Whang-Peng, J., Rogan, A. M., Green, W. R., and Ozols, R. F. (1983) *Cancer Res.* **43**, 5379–5389
- Plank, C., Oberhauser, B., Mechtler, K., Koch, C., and Wagner, E. (1994) *J. Biol. Chem.* **269**, 12918–12924
- Oeltmann, T. N., and Wiley, R. G. (1988) *Methods Enzymol.* **165**, 204–210
- Carroll, S. F., Barbieri, J. T., and Collier, R. J. (1988) *Methods Enzymol.* **165**, 68–76
- Carroll, S. F., and Collier, R. J. (1988) *Methods Enzymol.* **165**, 218–225
- Fiske, C. H., and Subbarow, Y. (1925) *J. Biol. Chem.* **66**, 375–400
- Ishida, T., Iden, D. L., and Allen, T. M. (1999) *FEBS Lett.* **460**, 129–133
- Hennessey, J. P. J., and Johnson, W. C. J. (1981) *Biochemistry* **20**, 1085–1094
- Böhm, G. (1997) *CDNN CD Spectra Deconvolution Software*, Version 2.1
- Memoli, A., Palermiti, L. G., Travagli, V., and Alhaique, F. (1999) *J. Pharmacol. Biomed. Anal.* **19**, 627–632
- Memoli, A., Palermiti, L. G., Travagli, V., and Alhaique, F. (1994) *J. Pharmacol. Biomed. Anal.* **12**, 307–312
- Galla, H. J., and Hartmann, W. (1980) *Chem. Phys. Lipids* **27**, 199–219
- Kendall, D. A., and MacDonald, R. C. (1982) *J. Biol. Chem.* **257**, 13892–13895
- Arigita, C., Zuidam, N. J., Crommelin, D. J., and Hennink, W. E. (1999) *Pharm. Res. (N. Y.)* **16**, 1534–1541
- Düzgünes, N., and Gambale, F. (1988) *FEBS Lett.* **227**, 110–114
- Wharton, S. A., Martin, S. R., Ruigrok, R. W., Skehel, J. J., and Wiley, D. C. (1988) *J. Gen. Virol.* **69**, 1847–1857
- Brasseur, R. (2000) *Mol. Membr. Biol.* **17**, 31–40
- Subbarao, N. K., Parente, R. A., Szoka, F. C. J., Nadasdi, L., and Pongracz, K. (1987) *Biochemistry* **26**, 2964–2972
- Olson, F., Hunt, C. A., Szoka, F. C., Vail, W. J., and Papahadjopoulos, D. (1979) *Biochim. Biophys. Acta* **557**, 9–23
- Bailey, A. L., Monck, M. A., and Cullis, P. R. (1997) *Biochim. Biophys. Acta* **1324**, 232–244
- Steinhauer, D. A., Wharton, S. A., Skehel, J. J., and Wiley, D. C. (1995) *J. Virol.* **69**, 6643–6651
- Nichols, J. W., and Deamer, D. W. (1980) *Proc. Natl. Acad. Sci. U. S. A.* **77**, 2038–2042
- Rosignol, M., Thomas, P., and Grignon, C. (1982) *Biochim. Biophys. Acta* **684**, 195–199
- Shangquan, T., Alford, D., and Bentz, J. (1996) *Biochemistry* **35**, 4956–4965
- Puyal, C., Maurin, L., Miquel, G., Bienvenue, A., and Philippot, J. (1994) *Biochim. Biophys. Acta* **1195**, 259–266
- Pecheur, E. I., Hoekstra, D., Sainte-Marie, J., Maurin, L., Bienvenue, A., and Philippot, J. R. (1997) *Biochemistry* **36**, 3773–3781
- Laczko, I., Hollosi, M., Vass, E., and Toth, G. K. (1998) *Biochem. Biophys. Res. Commun.* **249**, 213–217

<sup>2</sup> E. Mastrobattista, G. A. Koning, L. van Bloois, A. C. S. Filipe, W. Jiskoot, and G. Storm, unpublished results.